

libel, J. Phys. Chem. Solids **29**, 1797 (1968); also I. Camlibel, M. DiDomenico, Jr., and S. H. Wemple, *ibid.* (to be published).

¹⁷D. Berlincourt and H. Jaffe, Phys. Rev. **111**, 143 (1958). The c_{11} value is confirmed by this study.

¹⁸S. H. Wemple (unpublished).

PHYSICAL REVIEW B

VOLUME 1, NUMBER 11

1 JUNE 1970

Temperature and Field Dependence of the Weak Ferromagnetic Moment of Hematite*

C. W. Searle and G. W. Dean

Department of Physics, University of Manitoba, Winnipeg 19, Canada

(Received 3 October 1969)

Deviations from the expected temperature dependence of the weak magnetic moment m are explained by considering the microscopic differences between the dipole-dipole and single-ion contributions to the anisotropy energy.

INTRODUCTION

Hematite (α Fe₂O₃) is a well-known antiferromagnet with a rhombohedral crystal structure. It also possesses a weak spontaneous magnetization. With cooling it is found that there exists a certain temperature T_M , at which the spontaneous magnetization suddenly disappears.¹ Below T_M the antiferromagnetic axis coincides with the [111] direction, while above T_M the antiferromagnetic axis is in the (111) plane.² The origin of the weak ferromagnetic moment is due to the Dzialoshinskii-Moriya (DM) interaction^{3,4} which results in a slight canting of the sublattice magnetizations to produce a weak ferromagnetic moment. The expression for the Hamiltonian in the molecular field (MF) approximation is usually written as⁵

$$\epsilon = \lambda \vec{M}_1 \cdot \vec{M}_2 - \vec{D} \cdot (\vec{M}_1 \times \vec{M}_2) - \vec{H} \cdot (\vec{M}_1 + \vec{M}_2) + \epsilon_K, \quad (1)$$

where \vec{M}_1 and \vec{M}_2 are the sublattice magnetizations, λ is the MF constant, \vec{D} is the DM vector and is parallel to the [111] direction, \vec{H} is the applied field, and ϵ_K represents the anisotropy energy.

Searle⁶ has recently suggested, using symmetry arguments, that once the spins have been labeled according to their respective sublattices the sense of \vec{D} along the [111] direction is still undetermined. This then leads to the possibility of observing ferromagnetic domains which would not be associated with antiferromagnetic domains.⁷ This does not rule out the existence of ferro- and antiferromagnetic domains reported by Nathans *et al.*⁸ It was also stressed that \vec{D} should be replaced by $\langle \vec{D} \rangle$, where $\langle \dots \rangle$ means the appropriate statistical average. The expression for the weak magnetic moment m can then be written as

$$m = \langle H_D \rangle / H_e M. \quad (2)$$

Here $\langle H_D \rangle = \langle D \rangle M$, M is the magnitude of one of the

sublattice magnetizations, and $H_e = \lambda M$. Equation (2) implies that the ratio $m/M = \langle D \rangle / \lambda$ should decrease with increasing temperature. It was also suggested that the field-induced transition, for temperatures below T_M , might be described better using this statistical model than the usual MF approach where \vec{D} is assumed to be constant (such as in calculations by Cinader and Shtrikman⁹). The purpose of this experiment was to look for some of these effects using static magnetization measurements.

RESULTS

The upper curve in Fig. 1 indicates the temperature dependence of the normalized sublattice magnetization, M/M_0 . Values of M/M_0 are taken from

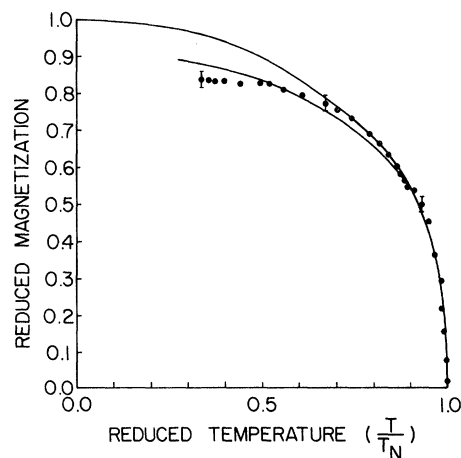


FIG. 1. Temperature dependence of the weak ferromagnetic moment of hematite. The upper curve represents the normalized temperature dependence of the sublattice magnetization, M/M_0 , the dots are the experimental data m/m_0 , while the lower curve is calculated from Eq. (6).

hyperfine field data obtained by van der Woude.¹⁰ It is assumed that the temperature dependence of the measured hyperfine field and M are the same. Experimental values of m/m_0 , where m_0 is a temperature-independent scaling factor, were obtained using a vibrating sample magnetometer. No value of m_0 can provide agreement between m/m_0 and M/M_0 over the entire temperature range. The experimental points m/m_0 are fitted to M/M_0 at $T/T_N = 0.85$ which emphasizes the difference in their temperature dependence and tends to fit the lower calculated curve.

The ratio $(m/m_0)/(M/M_0)$ is shown in Fig. 2. It is apparent that this ratio increases with T for a considerable range instead of decreasing. Thus the expected statistical behavior is absent or masked by some other effect. In fact, another effect must be present since if it were not this ratio should decrease with T or at most be temperature independent and equal to one as shown by the upper curve in Fig. 2.

Data presented in Figs. 3 and 4 show the results of the field-induced transition experiments. The magnetic field was applied in the (111) plane and was varied in magnitude. The temperature was maintained constant during each run, with a possible drift during the run of $\pm 0.06^\circ$. In Fig. 4 the dots are data obtained for increasing H , while the crosses are data obtained for decreasing H all taken during the same run at the same temperature. It can be seen that the applied field induces a sudden transition at a certain critical value H_c , where H_c increases with decreasing T . There is also no hysteresis associated with H_c . These experimental results are in complete agreement with those of Flanders and Shtrikman.¹¹

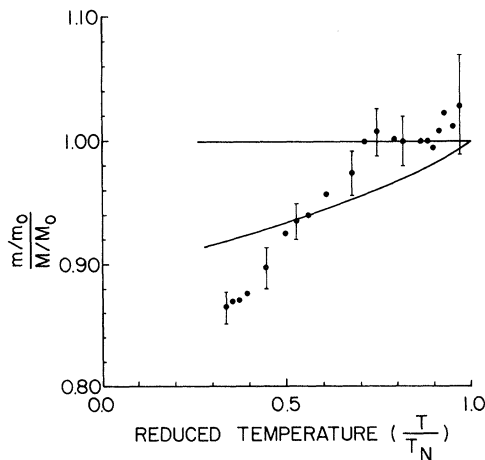


FIG. 2. Temperature dependence of $(m/m_0)/(M/M_0)$. The upper curve which is equal to 1 is the result of a MF calculation. The dots are experimental values, and the lower curve was calculated from the present model.

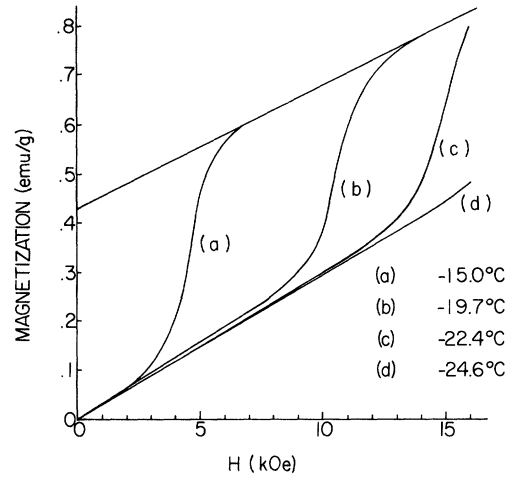


FIG. 3. Field induced transitions where the external magnetic field is applied in the (111) plane.

DISCUSSION

It appears that the experimental data can be described by the microscopic differences between the single-ion and dipole-dipole contributions to the anisotropy energy. No attempt will be made to solve this complicated problem but simplifying assumptions will be used in order to stress the interactions which are believed to be responsible for the experimental effects.

The spin Hamiltonian for α - Fe_2O_3 may be written to second order in the spin components as follows¹²:

$$\mathcal{H} = \sum_{j>k} [J_{jk}(\vec{S}_j \cdot \vec{S}_k) + \vec{d}_{jk} \cdot (\vec{S}_j \times \vec{S}_k) + \vec{S}_j \cdot K_{jk} \cdot \vec{S}_k] - \sum_j D_1 S_{jx}^2 \quad (3)$$

The first term is the isotropic superexchange interaction, the second term is the antisymmetrical spin coupling, the third term is the magnetic dipole interaction, and the fourth term is the single-ion anisotropy energy. In the following argument the second term is dropped (to be considered later), Eq. (3) is rewritten in terms of the MF approximation, and only the j th ion is considered. This yields

$$\mathcal{H}_j = -g\mu_B S_{jz} H_{ex} - D_1 S_{jx}^2 + D_2 \langle S_x \rangle S_{jx} \quad (4)$$

Here H_{ex} is the effective MF, the second term is the single-ion anisotropy energy, the last term is the magnetic dipole interaction (using essentially the same notation as Artman *et al.*¹³), and $\langle S_x \rangle$ represents the average spin polarization per ion of one sublattice in the x direction.

Figure 5 indicates the relation of the spin coordinate system to the crystal structure.

It is further assumed that the temperature vari-

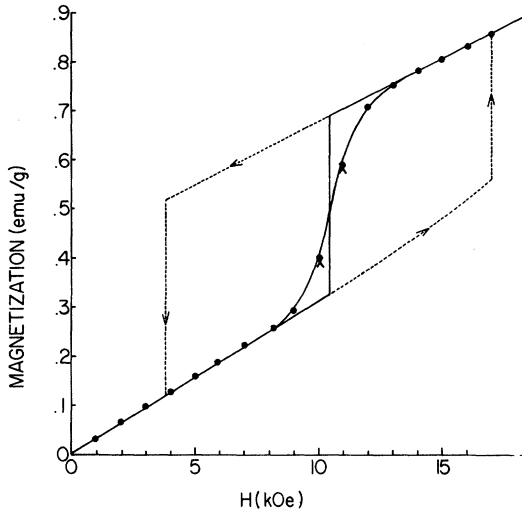


FIG. 4. Comparison of the data obtained in the field-induced transition experiment with a MF calculation. Equation (9) was used to express the anisotropy energy. $T = -19.7^\circ\text{C}$.

ation of the anisotropy energy can be taken into account by allowing D_1 and D_2 to be temperature dependent. This allows us to reach some important conclusions from a consideration of the ground-state spin function.

We consider the range $T > T_M$ where $D_2 > D_1$. According to the MF approximation, the antiferromagnetic axis is in the (111) plane and we will assume it is stabilized along the z direction by a very small anisotropy field. Equation (4) is expressed in terms of raising and lowering operators as follows:

$$\begin{aligned} \mathcal{H}_j = & -g\mu_B S_{jz} H_{ex} - \frac{1}{4} D_1 (S_{j+}^2 + S_{j+} S_{j-} + S_{j-} S_{j+} + S_{j-}^2) \\ & + \frac{1}{2} D_2 \langle S_x \rangle (S_{j+} + S_{j-}), \end{aligned} \quad (5)$$

where $S_{j\pm} = S_{jx} \pm iS_{jy}$. It is obvious that $|S_{jz}\rangle = |\frac{5}{2}\rangle$ is not the correct ground state for the following reasons. First, let us assume that it is the correct ground state then $\langle S_x \rangle$ must be zero, however, the second term in Eq. (5) mixes in some of the excited states $|\frac{3}{2}\rangle$ which, because of the exchange interaction, simply corresponds to a rotation of the quantization axis toward the $\pm x$ direction which would reduce the single-ion energy. We note that although neither the $\pm x$ direction is favored each sublattice must rotate as a unit to minimize the exchange energy. This means that now $\langle S_x \rangle = \pm | \langle S_x \rangle | \neq 0$. The third term in Eq. (5) is now different from zero and mixes in some of the excited states $|\frac{3}{2}\rangle$ which again will simply be a rotation of the quantization axis, this time back toward the (111) plane, which reduces the dipole energy.

Finally, we must have two possible antiferromagnetic states, which are represented in Fig. 5 by II_+ and II_- , and $\langle S_x \rangle_+ = -\langle S_x \rangle_-$. These two states will later be related to the two possible states suggested in Ref. 6 and for the rest of the argument we will assume this to be true. We can now understand why there is no statistical behavior associated with m . This follows because we now have two possible antiferromagnetic states slightly tilted out of the (111) plane by an angle $\pm\phi$ (this differs from Ref. 6, where it was assumed that only one antiferromagnetic axis existed and then to explain why $\bar{D} \neq 0$ an additional interaction was postulated which led to statistical effects). In a single domain the configuration will be either II_+ or II_- with no statistical mixing between them since they originate because of a long-range cooperative effect. An excitation from state II_+ to II_- will involve a large number of spins and correspond to the creation of a macroscopic domain. However, there is no reason why adjacent domains can not simultaneously be in the two different states.⁶

Within the bounds of the approximation we can estimate ϕ and therefore m since

$$m = DM_z/\lambda = (DM/\lambda) \cos\phi. \quad (6)$$

This is done by calculating the value of $\langle S_x \rangle$ required to produce no rotation of the antiferromagnetic axis to first order in the perturbed spin functions. This occurs when the gain of spin deviation associated with a rotation toward the [111] direction is equal to the loss of spin deviation associated with a rotation back toward the (111) plane or $(\frac{5}{2} - \frac{1}{2})a^2 = (\frac{5}{2} - \frac{3}{2})b^2$ which yields

$$2a^2 = b^2, \quad (7)$$

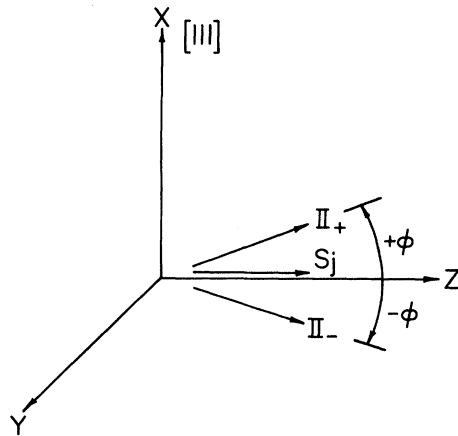


FIG. 5. Relation of the spin coordinate system to the crystal structure.

where
$$a = \frac{\langle \frac{1}{2} | \mathcal{J} C_j | \frac{5}{2} \rangle}{\langle \frac{5}{2} | \mathcal{J} C_j | \frac{5}{2} \rangle - \langle \frac{1}{2} | \mathcal{J} C_j | \frac{1}{2} \rangle}$$

and
$$b = \frac{\langle \frac{3}{2} | \mathcal{J} C_j | \frac{5}{2} \rangle}{\langle \frac{5}{2} | \mathcal{J} C_j | \frac{5}{2} \rangle - \langle \frac{3}{2} | \mathcal{J} C_j | \frac{3}{2} \rangle} .$$

From Eq. (5) we have

$$\langle \frac{1}{2} | \mathcal{J} C_j | \frac{5}{2} \rangle = -\frac{1}{4} D_1 (\sqrt{40}) ,$$

$$\langle \frac{3}{2} | \mathcal{J} C_j | \frac{5}{2} \rangle = \frac{1}{2} D_2 \langle S_x \rangle \sqrt{5} ,$$

$$\langle \frac{5}{2} | \mathcal{J} C_j | \frac{5}{2} \rangle \simeq -g \mu_B \frac{5}{2} H_{ex} ,$$

$$\langle \frac{3}{2} | \mathcal{J} C_j | \frac{3}{2} \rangle \simeq -g \mu_B \frac{3}{2} H_{ex} ,$$

and $\langle \frac{1}{2} | \mathcal{J} C_j | \frac{1}{2} \rangle \simeq -g \mu_B \frac{1}{2} H_{ex} .$

This then yields

$$a^2 = \frac{D_1^2 5}{8g^2 \mu_B^2 H_e^2} \quad \text{and} \quad b^2 = \frac{D_2^2 \langle S_x \rangle^2 5}{4g^2 \mu_B^2 H_e^2} .$$

Substitution of these values into Eq. (7) results in

$$\langle S_x \rangle^2 = (D_1/D_2)^2 .$$

Finally, we can write

$$\sin^2(\phi) = \langle S_x \rangle^2 / (\frac{5}{2})^2 = (D_1/D_2)^2 0.16 .$$

The calculated curve in Fig. 1 is Eq. (6) where ϕ was calculated according to the procedure above and D_1/D_2 is the ratio of the anisotropy energies.¹³ The lower curve in Fig. 2 is calculated by forming the ratio of m/m_0 , calculated from Eq. (6), to M/M_0 . It can be seen that the calculation provides a result which is the correct order of magnitude and also has the correct temperature dependence. Figure 2 indicates that the calculated curve agrees with the experimental data much better than the upper curve independent of any scaling factor and provides support for the interpretation outlined above.

The calculated curve in Fig. 4 is the result of adding a second-order term to the phenomenological expression for the anisotropy energy. We found this was the most reasonable way to describe the experimental results in agreement with Cinader *et al.*¹⁴ In this model ϵ_K in Eq. (1) is written as

$$\epsilon_K = K_1 \cos^2 \theta - K_2 \cos^4 \theta . \quad (8)$$

Here K_1 and K_2 are the first- and second-order coefficients for the expansion of the anisotropy energy and θ is the angle between the antiferromagnetic axis and the [111] direction. (It should be noted that this phenomenological description does not include the effects which were discussed earlier.) The transition was taken to be the point of equal energy between the ferromagnetic phase and the antiferromagnetic phase. This model does,

however, predict a hysteresis effect¹⁴ as indicated by the dashed curves in Fig. 4.

The reason no hysteresis was found is most likely due to imperfections such as impurities or dislocations (which are always present at finite temperatures). Associated with any dislocation will be regions of effective positive and negative pressures. It is well known that positive pressures shift T_M up and negative pressures shift T_M down.¹⁵⁻¹⁷ This means that when we approach the equal energy point (H either increasing or decreasing) some regions of the crystal will already be through the transition. These regions will then act as nucleating points which allow the entire crystal to go through the transition at the equal energy points and we expect no hysteresis to be associated with the transition.

The microscopic origin of K_2 is probably also related to quantum-mechanical effects. Kanamori and Minatono¹⁸ have shown that representing the single-ion energy as it appears in Eq. (4) by a term equivalent to the first term in Eq. (8) is only valid for small θ . In fact, they point out that, for large θ , K is complicated and depends upon the direction and magnitude of the applied field in the second- (and higher-) order perturbation terms. Therefore, we expect second- and higher-order terms in the expansion of the anisotropy energy. Although they will in general be small, they become important in the region where the first-order terms in the expansion of the anisotropy energy, arising from single-ion and dipole contributions, tend to cancel. This fact became very clear in the first part of this discussion where we found the phenomenological expansion of the anisotropy energy could not be used near T_M . This also tends to support the interpretation that microscopic differences in the contributions to the anisotropy energy lead to different temperature dependencies for m/m_0 and M/M_0 .

Finally, we want to relate the two antiferromagnetic states discussed here to the two states suggested in Ref. 6. We note that the states Π_+ and Π_- are related by a rotation of the angular momentum coordinate system through 180° around the z axis or we can write the following relation between the two states:

$$\begin{array}{cccc} \Pi_+ & & \Pi_- & & \Pi_+ & & \Pi_- \\ \langle S_z \rangle & = & \langle S_z \rangle & , & S_{jz} & = & S_{jz} , \\ \langle S_x \rangle & = & -\langle S_x \rangle' & , & \text{and} & S_{jx} & = & -S_{jx} , \\ \langle S_y \rangle & = & -\langle S_y \rangle & , & S_{jy} & = & -S_{jy} . \end{array} \quad (9)$$

Because of the spin-orbit coupling and assuming the the ground orbital state is nondegenerate¹² we may also write

$$\begin{aligned}
\Pi_+ & & \Pi_- \\
L_{jz} & = & L_{jz} , \\
L_{jx} & = & -L_{jx} , \\
L_{jy} & = & -L_{jy} .
\end{aligned} \quad (10)$$

This means we should be able to obtain the spin Hamiltonian for state Π_- from the spin Hamiltonian for state Π_+ by replacing the Π_+ operators and average values wherever they appear in the original Hamiltonian with Π_- average values and operators. Then the average value of the energy associated with an individual ionic spin [from Eq. (4)] can be shown to be

$$\begin{aligned}
\langle E_j \rangle_+ = \langle E_j \rangle_- = -g\mu_B \langle S_{jz} \rangle H_{ex} \\
- D_1 \langle S_{jx}^2 \rangle + D_2 \langle S_{jx} \rangle \langle S_{jy} \rangle ,
\end{aligned} \quad (11)$$

which means that although the two states have slightly different spin configurations they are degenerate. To complete the model we must show that $\vec{d}_{12(+)} = -\vec{d}_{12(-)}$, where 1 and 2 designate two ionic positions and \vec{d}_{12} is the vector leading to the antisymmetric interaction between them. Following Moriya's notation¹² the second-order perturbation energy which is bilinear in the spin-orbit coupling and the exchange interaction is written as follows:

$$\begin{aligned}
E_2 = \sum_m \left(\frac{\langle n | \lambda \vec{L}_1 \cdot \vec{S}_1 | m \rangle 2J(mn'mn') \vec{S}_1 \cdot \vec{S}_2}{E_n - E_m} \right. \\
+ \frac{2J(m'n'mn') \vec{S}_1 \cdot \vec{S}_2 \langle m | \lambda \vec{L}_1 \cdot \vec{S}_1 | n \rangle}{E_n - E_m} \\
+ \sum_{m'} \frac{\langle n' | \lambda \vec{L}_2 \cdot \vec{S}_2 | m' \rangle 2J(m'n'm'n) \vec{S}_1 \cdot \vec{S}_2}{E_{n'} - E_{m'}} \\
+ \left. \frac{2J(n'n'm'n) \vec{S}_1 \cdot \vec{S}_2 \langle m' | \lambda \vec{L}_2 \cdot \vec{S}_2 | n' \rangle}{E_{n'} - E_{m'}} \right) , \quad (12)
\end{aligned}$$

where n, n' represent the ground orbital states, m, m' represent the excited orbital states of the two ions 1 and 2, and $J(m'n'mn')$ is an exchange integral. We see that $\langle E_2 \rangle_+ = \langle E_2 \rangle_-$ by using Eqs. (9) and (10) so we finally see the two states are degenerate even when one includes the interaction which leads to canting. According to Moriya's calculation¹²

$$\begin{aligned}
d_{12} = 2i\lambda \left(\sum_m \frac{J(mn'mn')}{E_n - E_m} \langle n | \vec{L}_1 | m \rangle \right. \\
- \left. \sum_{m'} \frac{J(m'n'mn')}{E_{n'} - E_{m'}} \langle n' | \vec{L}_2 | m' \rangle \right) .
\end{aligned}$$

Symmetry arguments show \vec{d} is parallel to the [111] direction¹² which means we can rewrite the expression for \vec{d}_{12} as

$$\begin{aligned}
\vec{d}_{12} = 2i\lambda \left(\sum_m \frac{J(mn'mn')}{E_n - E_m} \langle n | L_{1x} | m \rangle \right. \\
- \left. \sum_{m'} \frac{J(m'n'mn')}{E_{n'} - E_{m'}} \langle n' | L_{2x} | m' \rangle \right) i_x . \quad (13)
\end{aligned}$$

Use of Eqs. (10) and (13) immediately leads us to the conclusion that $\vec{d}_{12(+)} = -\vec{d}_{12(-)}$ as suggested in Ref. 6.

CONCLUSIONS

All our experimental data can be described in terms of the microscopic differences between the single-ion and magnetic dipole contributions to the anisotropy energy. It is also suggested that near T_M (where the first-order contributions to the anisotropy energy from the two effects tend to cancel) higher-order terms in the phenomenological expression for the anisotropy energy should be there and are seen. Flanders¹⁹ has recently added a third-order term, and more can be expected if the experiment is refined and repeated.

It should also be mentioned that the model suggested in this paper is consistent with a recent experimental observation of Ozhogin *et al.*²⁰ They found that the sign of $\vec{D} \cdot \vec{I}$ was conserved, where $\vec{I} = (\vec{S}_1 - \vec{S}_2)$ describes the direction of the antiferromagnetic axis after labeling the spins. The sign of $\vec{D} \cdot \vec{I}$ is not conserved when \vec{D} is required to be uniquely determined in direction and magnitude after labeling the spins (the current view), unless $\alpha\text{Fe}_2\text{O}_3$ is not basically a uniaxial antiferromagnet.

An alternate model which should be considered would stress the fact that $\alpha\text{Fe}_2\text{O}_3$ is actually a four-sublattice antiferromagnet (see Herbert²¹). For temperatures $T > T_M$ the pairs of sublattices which tend to be parallel may split into two distinct sublattices each canting slightly toward the [111] direction with opposite senses. This possibility would also be consistent with our earlier arguments based on the microscopic differences between the dipole-dipole and single-ion contributions to the anisotropy energy, thus leading to a result similar to Eq. (6). This effect then could also describe our experimental results. It is also suggested that a microscopic calculation based on this four-sublattice approach might possibly lead to the current view that \vec{D} is uniquely determined in direction and magnitude after labeling the spins. It is concluded that a precise experiment is needed which can show whether our experiment indicates a slight inclination of the antiferromagnetic axis with respect to the (111) plane, or indicates four distinct sublattices.

*Work supported by a National Research Council of Canada Grant No. A2883.

¹F. J. Morin, *Phys. Rev.* **78**, 819 (1950); A. H. Morrish, G. B. Johnston, and N. A. Curry, *Phys. Letters* **7**, 177 (1963).

²C. G. Shull, W. A. Strauser, and E. O. Wollan, *Phys. Rev.* **83**, 333 (1951).

³I. Dzialoshinskii, *Zh. Eksperim. i Teor. Fiz.* **32**, 1547 (1957) [*Soviet Phys. JETP* **5**, 1259 (1957)].

⁴T. Moriya, *Phys. Rev.* **120**, 91 (1960).

⁵P. J. Besser, A. H. Morrish, and C. W. Searle, *Phys. Rev.* **153**, 632 (1967).

⁶C. W. Searle, *Phys. Rev. Letters* **21**, 741 (1968).

⁷J. A. Eaton, A. H. Morrish, and C. W. Searle, *Phys. Letters* **26A**, 520 (1968).

⁸R. Nathans, S. J. Pickart, H. A. Alperin, and P. J. Brown, *Phys. Rev.* **136**, A1641 (1964).

⁹G. Cinader and S. Shtrikman, *Solid State Commun.* **4**, 459 (1966).

¹⁰F. van der Woude, Ph.D. thesis, University of Groningen, Holland, 1966 (unpublished).

¹¹P. J. Flanders and S. Shtrikman, *Solid State Commun.* **3**, 285 (1965).

¹²T. Moriya, in *Magnetism I*, edited by G. T. Rado and H. Suhl (Academic, New York), pp. 97, 92, 93.

¹³J. O. Artman, J. C. Murphy, and S. Foner, *Phys. Rev.* **138**, A912 (1965).

¹⁴G. Cinader, P. J. Flanders, and S. Shtrikman, *Phys. Rev.* **162**, 419 (1967).

¹⁵C. W. Searle, *Phys. Letters* **25A**, 256 (1967).

¹⁶H. Umebayashi, B. C. Frager, and G. Shirane, *Phys. Letters* **22**, 407 (1966).

¹⁷T. G. Worlton, R. B. Bennion, and R. M. Brugger, *Phys. Letters* **24A**, 653 (1967).

¹⁸J. Kanamori and H. Minatono, *J. Phys. Soc. Japan* **17**, 1759 (1962).

¹⁹P. J. Flanders, *J. Appl. Phys.* **40**, 1247 (1969).

²⁰V. I. Ozhogin, S. S. Yakimov, R. A. Voskanyan, and V. Ya. Gamlickii, Institute of Atomic Energy Report No. IAE 1674, Moscow, 1968 (unpublished).

²¹D. C. Herbert, Ph.D. thesis, London University, 1968 (unpublished).

Harmonic Generation and Parametrically Coupled Spin Waves in Yttrium Iron Garnet*

J. D. Bierlein[†] and Peter M. Richards

Department of Physics, University of Kansas, Lawrence, Kansas 66044

(Received 30 December 1969)

Second-harmonic generation and ferromagnetic resonance have been investigated in spheres of yttrium iron garnet (YIG) as a function of incident power above the threshold for excitation of z -directed spin waves by the second-order Suhl instability. The fundamental frequency was 8.42 GHz and the temperature 300 °K. The second-harmonic power output $P_{2\omega}$ has the following features above threshold: (a) $P_{2\omega}$ goes through a minimum and then a maximum as a function of incident power; (b) the line profile of $P_{2\omega}$ versus dc field H shows two and then three peaks; (c) sufficiently far above threshold, $P_{2\omega}$ initially increases after the pulse of incident power is turned off. None of these effects is correlated with unusual behavior of the transverse magnetization, which always increases with power above threshold, has a single resonance line, and begins to decay as soon as incident power is turned off. The results are explained in terms of parametric coupling between the initially excited z -directed spin waves and other spin waves, with explicit account taken of the ensuing phase relations. These tend to make the other spin waves interfere destructively with the uniform mode ($k=0$) in their contribution to $P_{2\omega}$. In this way, quantitative agreement between theory and experiment is obtained with reasonable values for two adjustable parameters. Coherent phase relations between the interacting spin waves are essential for an understanding of the results. If all $k \neq 0$ magnon interactions are lumped into effective relaxation rates, it is possible to explain the transverse resonance data, but not the second-harmonic effects.

I. INTRODUCTION

Since the explanation by Suhl¹ of the premature saturation of ferromagnetic resonance observed by Bloembergen and Wang,² it has been known that spin waves of nonzero wave vector are excited in conventional (transverse pumping) ferromagnetic resonance experiments. This excitation occurs through parametric coupling of the uniform mode to a pair of spin waves with wave vectors \vec{k} and

$-\vec{k}$. When the uniform mode reaches a critical amplitude determined by the coupling strength and spin-wave relaxation rate, the pair \vec{k} and $-\vec{k}$ is excited to a very large amplitude. Further growth of the uniform mode amplitude is inhibited, thus causing the observed saturation.

In its original and most elementary form, theory predicts the uniform-mode amplitude to stay constant above threshold which results in the rf susceptibility declining as $1/h$, where h is the driv-